

# Experimental Study of the Behavior of a Hybrid Ejector-based Air-conditioning System with R134a

Hao Wang, Wenjian Cai, Youyi Wang, Jia Yan, Lei Wang

**Abstract**—A hybrid ejector-based air-conditioning system which combines a vapor compression cycle and a ejector refrigeration cycle was developed. The waste heat energy from automobile is applied as driven source towards ejector refrigeration cycle. Two ejectors with different mixing chamber diameters are applied separately for performance test and the system is operated under different working modes. The effect of generating, condensing and evaporating pressure on system performance are studied experimentally. The effect of ejector geometry parameters on ejector performance is also investigated. The performance comparison between two working modes is made and the results indicate that 1) the performance of proposed system is sensitive to the three pressures; 2) the coefficient of performance (COP) of hybrid ejector-based air-conditioning system is around 34% higher than that of conventional compressor based system which implies a potential energy saving ability of proposed hybrid system.

**Keywords**—Ejector, Performance evaluation, Low grade heat energy, Hybrid mode, Coefficient of performance

## I. INTRODUCTION

Although ejector has been invented for decades which is earlier than compressor, the progress of ejector based refrigeration system is slow compared with vapor compression system. The reason for this is that the efficiency of vapor compression system is much higher than that of ejector refrigeration system. [1]-[5] However, due to the deteriorating environment caused by massive CO<sub>2</sub> emission and declining global storage of fossil fuel resources, ejector refrigeration system have regained research interests. The distinctive characteristic of ejector refrigeration system is its ability to utilize low grade heat energy which can be easily acquired from automobile waste gas, solar radiation, industrial process and geothermal energy. [6]- [6] Moreover, because of the application of ejector, the system possesses many advantages, such as passive device (no moving components), durable life span, little maintenance cost and high reliable. The main restriction of prevalence of ejector refrigeration system is its relative low efficiency compared to vapor compression system.

To have insightful comprehension on the effect of ejector in the whole system and to improve the efficiency of ejector refrigeration system, many studies have been conducted including performance evaluation towards variety of systems. Pounds [11] investigated the effect of nozzle size, axial nozzle location, high-temperature evaporator temperature and refrigeration temperature by conducting experiment of an ejector refrigeration system. The author found that an optimum nozzle location exists and could produce a maximum coefficient of performance (COP). The results showed that ejector refrigeration system can achieve a COP of 1.7 which demonstrated a very promising future. Yin Hai Zhu [11] conducted experiments with an integrated ejector cooling system to analyze the system performance under design conditions. The results indicated that 9.1% COP improvement can be achieved using R22. The author then compared the system performance with the variations of 5 important parameters. The comparison illustrated that the refrigerant with high generator discharge temperature can improve the COP of the ejector cycle effectively. Yan Jia [12][13] studied the effects of ejector area ratio on system performance. An ejector with replaceable nozzle was applied in order to obtain the optimum area ratios under operation conditions. The consequence showed that the optimum area ratios fall in the range from 3.69 to 4.76 which are smaller than other previous studies. Also the operating conditions had great impact on the influence of area ratio. Chen Jianyong [14] investigated experimentally the influence of different temperatures on ejector refrigeration system performance using R123 and R141b. The results indicated that the condenser temperature had more influence than the generator and evaporator temperature on the area ratio and the entrainment ratio in the ejector. Additionally, the author concluded that area ratios need to keep up the pace with the variation of entrainment ratio as operating conditions are changed. Thus, a variable-geometry ejector seemed to be a very promising alternative to guarantee the optimum conditions of ejector

Wang Hao is with the school of Electrical and Electronic Engineering, Nanyang Technological University, Singapore, 639798 Singapore. (e-mail: wang0818@e.ntu.edu.sg).

Cai Wenjian is with the school of Electrical and Electronic Engineering, Nanyang Technological University, Singapore, 639798 Singapore. (e-mail: ewjcai@ntu.edu.sg).

Wang Youyi is with the school of Electrical and Electronic Engineering, Nanyang Technological University, Singapore, 639798 Singapore. (e-mail: eyywang@ntu.edu.sg).

40 refrigeration system.

41 The refrigerant used in the system is also of concerned. F.Wang [15] conducted a theoretical study on the evaluation of  
 42 environment-friendly refrigerants with similar normal boiling points in ejector refrigeration cycle. Totally eight different kinds of  
 43 refrigerants were studied comparatively. Entrainment ratios of ejector, system COP, pump power et al. of refrigerants were  
 44 recorded and analyzed. The result shows that R134a and R152a have similar normal boiling points and give better performance and  
 45 their COP were stable under different operation status. Besagni Giorgio [16] investigated the performance of heat driven ejector  
 46 refrigeration system using refrigerant R134a, R600 and R601. The effect of generator, evaporator and condenser temperature over  
 47 the entrainment ratio and COP had been studied under typical operating conditions of low grade energy sources. From the result  
 48 obtained, it can be observed that the working fluids had a great impact on the ejector performance and each refrigerant had its own  
 49 range of operating conditions. The optimum generating temperature for R134a is lower than others and is suitable for generator  
 50 temperature between 70 and 100 °C. Besides, R134a has several advantages over other refrigerants: 0 ozone depletion potential and  
 51 relative lower global warming impact. Thus, R134a is chosen as the working fluid in our system.

52 In other studies, Boumaraf [17] presented a novel ejector expansion refrigeration cycle which applied two evaporators using  
 53 ejector as a throttling valve. The constant area mixing model was applied to perform thermodynamic analysis of the new system.  
 54 Both R134a and its potential substitute R1234yf was applied for investigation. It was found that the novel system had a significant  
 55 improvement in COP for both R134a and R1234yf, moreover, the COP improvement of the new system using R134a was higher  
 56 than that of R1234yf and was able to achieve more than 17% increase at certain condensing temperature.

**Nomenclature**

D	Diameter (mm)	<i>Subscripts</i>	
L	Length (mm)	t	Nozzle throat
<i>h</i>	Specific enthalpy (kJ/kg)	e	Nozzle exit
<i>s</i>	Specific entropy (kJ/kg·K)	m	Mixing chamber
T	Temperature (°C)	f	Diffuser
P	Pressure (bar)	A,B	Ejector A, B
W	Power consumption (kW)	com	Compressor
<i>m</i>	Mass flow rate (kg/s)	con	Condenser
<i>n</i>	coefficient	eva	Evaporator
Q	Heat load (kW)	SF	Secondary flow
<i>c</i>	coefficient	WF	Working flow
$\eta$	Ideal isentropic efficiency	sat	Saturation condition
A	Area (m <sup>2</sup> )	s	Secondary flow
$\gamma$	Specific heat ratio	m	Mixing flow
$\psi$	Isentropic efficiency	isen	isentropic
R	Ideal gas constant	p	Primary flow
<i>V</i>	Velocity (m/s)		
H	Heat transfer coefficient	<i>Superscripts</i>	
<i>v</i>	Kinematic viscosity	<i>e,n</i>	Coefficient
$\mu$	Absolute viscosity		
<i>k</i>	Thermal conductivity		
<i>b</i>	Coefficient		
$\rho$	Density (kg/m <sup>3</sup> )		

57 Chen Lin [18] proposed an experimental investigation of the adjustable ejector in a multi-evaporator refrigeration system. Two  
 58 parameters namely pressure recovery ratio (PRR) and relative pressure recovery ratio (RPRR) are measured to evaluate the system  
 59 performance. The results show that the proposed system can be a promising approach to save energy significantly. Moreover, the  
 60 decreasing of the primary cooling load will lead to the reduction of both PRR and RPRR. Meibo Xing [19] explored the extent of  
 61 COP improvement of a novel vapor-compression refrigeration cycle with mechanical sub-cooling using an ejector. The author  
 62 developed a mathematical model to predict the performance of the cycle by using R404A and R290. The results suggest that the  
 63 ejector sub-cooled cycle is better than that of the conventional cycle. The novel cycle would achieve volumetric refrigeration  
 64 capacity improvement of 11.7% with R404A and 7.2% with R290. Furthermore, the COP improvement of novel cycle was 9.5%  
 65 with R404A and 7.0% with R290. In addition, the improvement of COP and cooling capacity majorly depended on the operation  
 66 conditions of the ejector. Huang [20][21] which was capable of making use of waste energy from vapor refrigerant under  
 67 superheated state. From the result they obtain, 15.4% COP improvement can be realized averagely while the maximum can reach to  
 68 24.5%. Kursad Ersoy [20] applied an ejector for expansion purpose instead of an expansion valve for expansion work recovery in

69 a vapor compression cycle. The author experimentally investigated the COP values for both conventional and ejector systems  
70 under same external conditions. The data obtained demonstrated that the system with ejector as the expander had better  
71 performance than the conventional one and the COP improvement was 6.2%-14.5% within an error of approximately 10%.  
72 Currently, no literature has been found on attempting to connect ejector and evaporator with compressor directly.

73 To fill this blank, we have proposed a hybrid system in which the evaporator outlet is connected directly to ejector secondary  
74 inlet via a variable speed compressor. A series of experiment tests are conducted in order to 1) investigate the effect of primary  
75 pressure, evaporating pressure and back pressure on COP and entrainment ratio; 2) to investigate the ejector mixing chamber effect  
76 on COP by using ejectors with different geometry parameters and 3) to compare the performance of both general mode and hybrid  
77 mode. The results show that the performance of the proposed system is very sensitive to three pressures of cycle and relatively  
78 promising COP improvements are achievable which imply a huge potential in the future.

## 79 II. EXPERIMENT DESCRIPTION

80 As shown in Figure 1, the proposed system is consisted of two sub-cycles: a vapor compression cycle and an ejector refrigeration  
81 cycle. The system can be operated under two different working modes, namely general (or compressor only) mode and hybrid  
82 mode (combination of compressor and ejector), by switching control valves installed in the refrigeration loop. Under the hybrid  
83 mode, compressor is in series connected with the ejector secondary inlet which is the evaporator outlet.

84 The rationale for such arrangement is that the suction effect generated by ejector helps reducing the compression ratio of the  
85 compressor which in turn reduces the power consumption of compressor. In addition, the diffuser section of ejector will decelerate  
86 the discharge refrigerant and increases its pressure to the condensing pressure which helps improve the efficiency of condenser.  
87 Thus the overall COP of system can be improved.

88 A photograph of experimental platform is shown as in Fig. 1, the whole system is consisted of following components:

- 89 • A generator;
- 90 • An electric evaporator;
- 91 • An air-cooled condenser;
- 92 • An ejector;
- 93 • A liquid receiver;
- 94 • A liquid pump;
- 95 • An electronic expansion valve (EEV);
- 96 • A compressor;
- 97 • A monitoring and control system using LabVIEW.

98 The schematic diagram of the system is shown in Fig. 2.



Fig. 1. Photograph of hybrid ejector refrigeration system

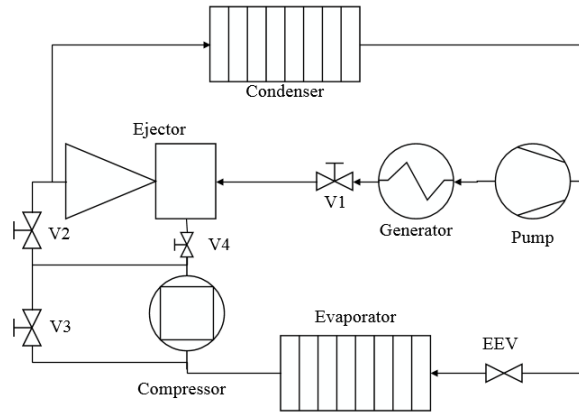


Fig. 2. Schematic diagram of hybrid ejector refrigeration system

TABLE I. OPERATION INFORMATION FOR DIFFERENT MODES

Different Modes	Operation details
General Mode	V1, V3, V4 off, V2 on
Ejector Mode	V2 off, V1, V3, V4 on
Hybrid Mode	V2, V3 off, V1, V4 on

The  $p-h$  chart of hybrid mode operation is shown in Fig.3.

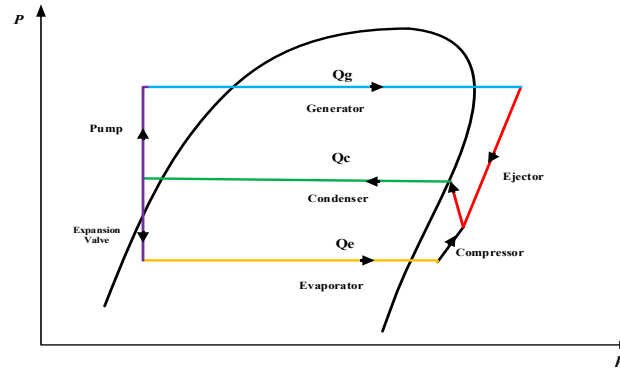


Fig. 3.  $p-h$  chart of hybrid mode operation

The generator consists of a vapor collection tank, a tubular heater immersed in the tank and a temperature-controlled conduction oil bath. The oil bath is heated by an electric heater with maximum power output of 8 kW. The temperature of the hot oil is maintained at 120°C with deviation of  $\pm 0.5^\circ\text{C}$  by a PID controller. The electric evaporator with maximum power output of 3 kW is installed to accurately measure the system cooling capacity. The air-cooled condenser has rated condensing load of 15.6 kW and the vapor refrigerant is from the diffuser of ejector. The liquid pump is located at the bottom of the platform in case of cavitation. The speed of the pump is adjusted via a control device. The EEV is impelled by a step motor which is controlled by a PID controller. The inverter compressor is applied after the evaporator in order to raise the secondary flow pressure to designed value. To avoid heat losses and gains, all tubes are covered with thick glass fiber wool that has an aluminum foil layer on its outer surface. The monitoring and control panel are built based on LabVIEW.

In addition, eight hand valves are installed which allow the system being operated under different modes; two flow meters with different measuring range are placed at certain position to accurately measure the primary and secondary mass flow rate; several pressure and temperature sensors installed in the system are showed in following table. Since the range of generating pressure is 10~23bar, the pressure sensor with range from 0~40bar is applied at ejector primary side. These sensors are widely used among industrial fields for their high accuracy and steady performance. Therefore, no further calibration is needed.

TABLE II. DETAILS OF MEASUREMENT DEVICES

Different Sensors	Instrument	Unit of measurement	Accuracy	Range
Temperature	PT1000 platinum resistance sensors	°C	±0.05	-50~150
Pressure	Huba OEM piezoelectric pressure transmitters	Bar	±0.01	0~15
Pressure	Huba OEM piezoelectric pressure transmitters	Bar	±0.02	0~40
Flow rate	Yokogawa RAMC rotor flow meters	L/h	±0.32	0~20
Flow rate	Yokogawa RAMC rotor flow meters	L/h	±1.92	0~120

123 The experimental plant was usually brought to steady state condition within 40mins after the inputs were changed. Data  
 124 collection process was begun as soon as the system stabilized. The refrigerant enthalpies are determined from measured  
 125 temperature and pressure values according to NIST database. The total expanded uncertainties for the airside heat transfer rate  
 126 measurements are ±1.5%. The total expanded uncertainties for the refrigerant side heat transfer rate measurements are ±3.5% for  
 127 the condenser and ±5% for the generator, with the biggest contributor being the uncertainties in the thermodynamic property  
 128 estimation calculations [23].

129 Fig.4 and Fig.5 show the dimensions of two ejectors used in the experiments. The detail parameters are listed as follow:

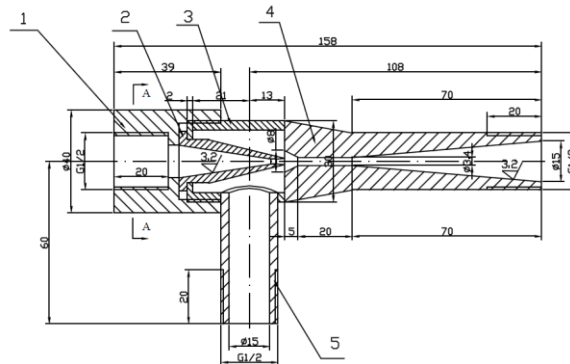


Fig. 4. Schematic diagram of ejector A

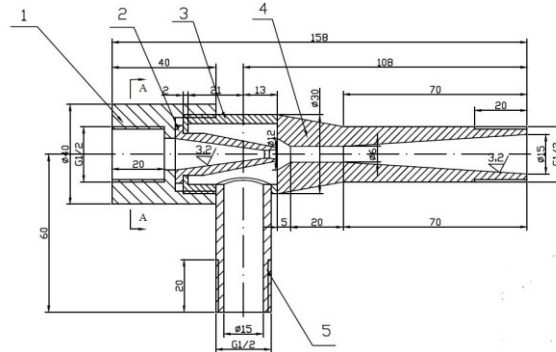


Fig. 5. Schematic diagram of ejector B

130  
131

132  
133

- Diameter at nozzle throat  $D_{tA}=1.6\text{mm}$ ,  $D_{tB}=3\text{mm}$ .
- Diameter at nozzle exit  $D_{eA}=2.3\text{mm}$ ,  $D_{eB}=3.8\text{mm}$ .
- Mixing chamber diameter  $D_{mA}=3.4\text{mm}$ ,  $D_{mB}=6\text{mm}$ .
- Diffuser exit diameter  $D_{fA}=D_{fB}=15\text{mm}$ .
- The distance between nozzle exit and the mixing chamber inlet  $NXP_A=NXP_B=5\text{mm}$ .
- Mixing chamber length  $L_{mA}=L_{mB}=20\text{mm}$ .
- Diffuser length  $L_{fA}=L_{fB}=70\text{mm}$ .
- Nozzle divergent section length  $L_{nA}=4\text{mm}$ ,  $L_{nB}=5\text{mm}$ .

142 The ejector consists of four parts: *The nozzle, the suction chamber, the mixing chamber and the diffuser.*

143 The working principle of the ejector is briefly described below:

144 The primary flow (sometimes referred as motive flow) enters the ejector with a subsonic velocity. It then goes through a  
 145 converging-diverging section. During the converging part, it is accelerated to high velocity and the pressure is reduced based on  
 146 Bernoulli's principle. The velocity reaches sonic with Mach number equals to 1 at the nozzle throat and the flow chokes. When it  
 147 continues passing through the diverging part, the velocity increases again and reaches supersonic. A very low pressure region  
 148 (sometimes referred as vacuum region) is generated in the suction chamber due to this high speed primary flow. Therefore, the  
 149 secondary flow from the evaporator is entrained by this suction force. The two flows then mix, compress and will generate several

150 shocks in the mixing chamber [24]. Generally speaking, there are two kinds of mixing chamber, a constant pressure type and a  
 151 constant area type. Each one has its own character, but the constant area type is more famous because of its simplicity of  
 152 manufacturing. The shock causes a sudden reduction in velocity and thereby an abrupt increase in pressure. As the mixing flow  
 153 emerges from mixing chamber, it goes through another pressure recovery process in the diffuser. The kinetic energy is converted  
 154 into potential energy. Finally, the pressure of mixture reaches the corresponding condensing pressure.

155 The design operating conditions of the system are: condensing pressure 9bar, evaporating pressure 3.5bar and generating  
 156 pressure 22bar. The design cooling capacity is 1.5kW. The experiment conditions are listed in table III. Particularly, the tests were  
 157 carried out from 9<sup>th</sup> Aug 2013 to 2<sup>nd</sup> May 2014 on every weekday 2pm in Singapore and the test duration was 3 hours per day.

158 TABLE III. OPERATING CONDITIONS OF THE SYSTEM

Operating Condition	Value
Ambient temperature (°C)	33~34
Condensing pressure (bar)	8~12
Evaporating pressure (bar)	2.5~4.5
Generating pressure (bar)	10~25
Compressor frequency (Hz)	30~50
EEV opening ratio ( $\omega$ )	30%~60%

159

### 160 III. SYSTEM PERFORMANCE ANALYSIS

161 The proposed hybrid system is a combination of a conventional vapor compression cycle and an ejector cycle. The governing  
 162 equations are based on conservation of energy and mass for each component in two sub-cycles.

#### 163 A. Compressor

164 Since the compression process happens rapidly, it is often assumed to be adiabatic. Based on NIST database, the enthalpy and  
 165 entropy of the refrigerant at compressor inlet are determined by the compressor inlet temperature and pressure as [26]:

166  
 167 
$$h_{com,inlet}, s_{com,inlet} = f(T_{com,inlet}, P_{com,inlet}) \quad (1)$$

168 The enthalpy of refrigerant at compressor outlet for the isentropic process is:

169  
 170  
 171 
$$h_{com,outlet,isen} = f(s_{com,outlet,isen}, P_{com,outlet}) \quad (2)$$

172  
 173 where  $s_{com,outlet,isen} = s_{com,inlet}$

174 The actual enthalpy at compressor outlet is:

175  
 176  
 177 
$$h_{com,outlet} = h_{com,inlet} + \frac{(h_{com,outlet,isen} - h_{com,inlet})}{\eta_c} \quad (3)$$

178 where  $\eta_c$  is the isentropic efficiency of compression process.

179 The power consumption of compressor can be calculated as:

180  
 181  
 182 
$$W_{com} = \dot{m} (h_{com,outlet} - h_{com,inlet}) \quad (4)$$

183

184 The heat transfer process mainly happens within two components: condenser and evaporator. Since the operation principle of  
 185 condenser and evaporator are similar, only condenser is selected as an illustration. A condensing process majorly consists of two  
 186 loops: the refrigerant loop and secondary fluid loop. In the refrigerant loop, the heat is transferred from refrigerant fluid to  
 187 secondary fluid through metal tube wall due to temperature difference between the two fluids in the manner of conduction. The  
 188 amount of heat transfer can be obtained by multiplying the refrigerant mass flow rate with enthalpy difference between inlet and  
 189 outlet. In the secondary fluid loop, the heat transfer is a single-phase forced convection process. Based on Newton's cooling law,  
 190 the convective heat transfer can be expressed as:

191  
192 
$$Q = HA\Delta T \quad (5)$$

193  
194 where  $H$  is the average convective heat transfer coefficient,  $A$  is the condenser surface are and  $\Delta T$  is the average temperature  
195 difference between metal tube wall and the secondary fluid, respectively.

196 The convective heat transfer  $H$  is usually determined empirically by a set of dimensionless fluid properties. For instance, the heat  
197 transfer coefficient of forced convection process can be expressed as:

198  
199 
$$\frac{Hd}{k} = C\left(\frac{Vd}{\nu}\right)^e\left(\frac{\mu c_p}{k}\right)^n \quad (6)$$

200  
201 where  $d$  is characteristic length,  $\nu$  is the kinematic viscosity,  $\mu$  is the absolute viscosity,  $c_p$  is the specific heat at constant pressure,  
202  $C, e$  and  $n$  are coefficients.

203 Since mass flow rate can be written as:

204  
205 
$$\dot{m} \quad (7)$$

206  
207 Substituting equation (7) into (6), after rearrangement and combination, we can obtain:

208  
209 
$$H = b\dot{m} \quad (8)$$

210  
211 where under steady state condition, the viscosity, thermal conductivity and specific heat are approximately constants. According to  
212 the principle of energy balance, the heat transfer of refrigerant side is equal to that of secondary fluid side. Combining the heat  
213 transfer of two loops and applying the Levenberg-Marquardt method, the  $H$  can be determined.

#### 214 B. Condenser

215 The condenser applied is air-cooled type. The enthalpy of refrigerant at condenser inlet is determined as:

216  
217 
$$h_{con,inlet} = f(T_{con,inlet}, P_{con,inlet}) \quad (9)$$

218  
219 Since the condensing process is assumed to be isobaric, the pressure remains constant, also the refrigerant is assumed to be  
220 saturated liquid at condenser exit:

221  
222 
$$h_{con,outlet} = f_{sat}(P_{con,outlet}) \quad (10)$$

223  
224 where  $P_{con,outlet} = P_{con,inlet}$

225 The heat load for condenser is then:

226  
227 
$$Q_{con} = \dot{m} (h_{con,inlet} - h_{con,outlet}) \quad (11)$$

#### 229 C. Evaporator

230 According to the hybrid evaporator model, the cooling capacity can be determined as [26]:

231  
232 
$$Q_{eva} = \dot{m}_s \left( h_{vap} - h_{eva,inlet} \right) \quad (12)$$

233  
234 where  $c_1, c_2$  and  $e$  are constant coefficients to be determined,  $h_{vap}$  and  $h_{eva,inlet}$  are the specific saturated vapor enthalpy and  
235 refrigerant enthalpy at evaporator inlet, respectively.  $T_{SF,inlet}$  and  $T_{sat}$  are secondary flow inlet temperature and saturated temperature  
236 of refrigerant,  $\dot{m}_s$  and  $\dot{m}_{SF}$  are mass flow rate of refrigerant and secondary flow.

237 The temperature can be obtained by the sensors installed. The specific enthalpy of refrigerant at evaporator inlet can be obtained  
238 through:

239

$$240 \quad h_{eva,inlet} = f(T_{eva,inlet}, P_{eva,inlet}) \quad (13)$$

241

242 *D. Pump*

243 The pump is not an isentropic process. The actual refrigerant enthalpy at the pump outlet can be obtained as:

244

$$245 \quad h_{pump,outlet} = h_{pump,inlet} + \frac{(h_{pump,outlet,isen} - h_{pump,inlet})}{\eta_{pump}} \quad (14)$$

246

247 where  $\eta_{pump}$  is the ideal isentropic efficiency of pump process. The thermodynamic conditions of refrigerant at pump inlet are the same as that at condenser outlet.

248 The enthalpy of the refrigerant at pump outlet for an isentropic process is:

249

$$251 \quad h_{pump,outlet,isen} = f(s_{pump,outlet,isen}, P_{pump,outlet}) \quad (15)$$

252

253 where  $s_{pump,outlet,isen} = s_{con,outlet}$ 

254 The power consumption of the liquid pump can be calculated as:

255

$$256 \quad W_{pump} = \dot{m} (h_{pump,outlet} - h_{pump,inlet}) \quad (16)$$

257

258 *E. Ejector*

259 The performance of ejector is influenced by both its geometric parameters and operation conditions. The entrainment ratio which is defined as the ratio of secondary mass flow rate to primary flow rate is usually applied to evaluate the ejector performance. The primary flow is often assumed to be choked in the primary nozzle, and under that condition as well as ideal gas assumption, the mass flow rate of primary flow can be given by [27]:

263

$$264 \quad \dot{m}_p = A_1 \sqrt{\frac{\gamma P_p}{R_g T_p}} \left( \frac{1 + \gamma}{2} \right)^{\frac{1 + \gamma}{2 - 2\gamma}} \quad (17)$$

265

266 where  $P_p$  and  $T_p$  are the stagnation pressure and temperature of the primary flow at the nozzle inlet,  $A_1$  is the area of nozzle throat,  $R_g$  is the ideal gas coefficient,  $\gamma$  is the specific heat ratio of vapor refrigerant and  $\psi_p$  is the isentropic coefficient of compressible flow, respectively.

269 The mass flow rate of secondary flow is more complicated to determine than primary flow. Based on shock circle model, it can be expressed as [28]:

270

$$272 \quad \dot{m}_s = \frac{\dot{m}_p V_{pm,inlet}}{V_{sm,inlet}} \left[ \frac{n D_m^2}{4n + 4} \left( 1 - \frac{D_{pm,inlet}}{D_m} \right)^{1 + \frac{1}{n}} - \frac{n D_m^2}{8n + 4} \left( 1 - \frac{D_{pm,inlet}}{D_m} \right)^{2 + \frac{1}{n}} \right] \quad (18)$$

273

274 where  $P_s$  is the stagnation pressure of the secondary flow at ejector inlet,  $V_{pm,inlet}$  and  $T_{sm,inlet}$  are the primary flow velocity and secondary flow temperature at mixing chamber inlet,  $D_m$  and  $D_{pm,inlet}$  are the diameter of mixing chamber and diameter of primary flow choke circle at mixing chamber inlet, respectively.

277 Hence, the entrainment ratio can be obtained as:

278

$$279 \quad \omega = \frac{\dot{m}_s}{\dot{m}_p} \quad (19)$$

280

281 The performance of the refrigeration system can be evaluated based on the coefficient of performance (also short as COP) which is defined as the cooling capacity generated to the power consumption the system need. The coefficient of performance of the proposed hybrid system is:

284

285 
$$COP_{hybrid} = \frac{Q_e}{W_{pump} + W_{com} + W_{gen}} \quad (20)$$

286  
287 The power consumption of generator is obtained by power meter installed.

288 And for the coefficient of performance of the conventional vapor compression system, it is expressed as:

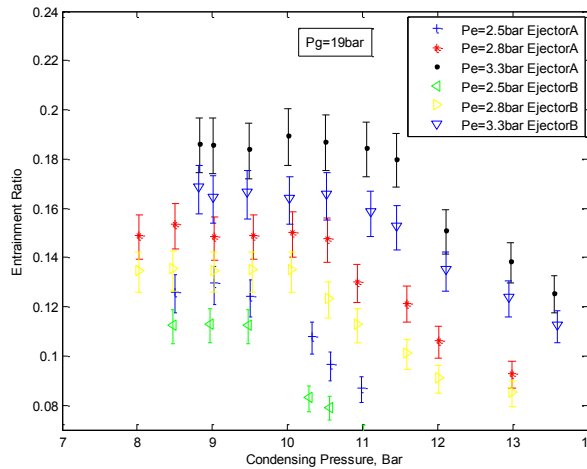
289  
290 
$$COP_{general} = \frac{Q_e}{W_{com}} \quad (21)$$

291 IV. EXPERIMENT RESULTS AND DISCUSSION

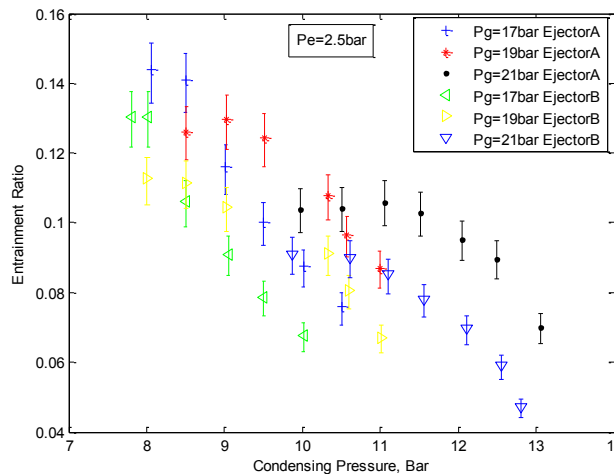
292 The major objective of this experiment is to investigate the effect of condenser, evaporator and generator pressure on the system  
293 performance with ejectors of different mixing chamber diameter. The controlling variables method is applied that means when  
294 investigating one particular parameter, the others remain constant. For instance, when investigating the back pressure effect on  
295 entrainment ratio, both generating pressure and evaporating pressure are kept constant. Also, the comparison between conventional  
296 vapor compression cycle and proposed hybrid cycle is of our interest. The operating conditions for two cycles are the same, only  
297 the structure difference is investigated. In order to mitigate the influence of random error, each experimental point is the average  
298 value of 50 experiment data. Moreover, based on accuracy of experimental apparatus and principle of error transfer, the relative  
299 error for entrainment ratio is 6.7%, for cooling capacity is 10.1% and for COP is 13.3%.

300 A. Effect of back pressure on entrainment ratio

301 The condensing pressure (back pressure) is closely related to entrainment ratio and is affected by ambient condition which is  
302 impossible to adjust compared with evaporating and generating pressures.



303  
304 Fig. 6. Variation of entrainment ratio with condensing pressure under constant generating pressure  
305



306  
307 Fig. 7. Variation of entrainment ratio with condensing pressure under constant evaporating pressure

308 The experiments are conducted under different conditions so that the relationship between critical back pressure and evaporating

(or generating) pressure can be obtained. In order to more intuitively reveal the variation trend of entrainment ratio under different operation conditions, experimental points are connected with lines. Fig.6 shows Variation of entrainment ratio with condensing pressure under constant generating pressure, it can be seen that 1) under constant evaporating ( $P_e$ ) and generating pressure ( $P_g$ ), entrainment ratio remains constant before condensing pressure increases to a certain value, 2) as condensing pressure increases, the entrainment ratio drop sharply. The reason for this critical condensing pressure is that when condensing pressure ( $P_c$ ) is lower than critical pressure, the mixed flow is choked within mixing chamber. Therefore, the mass flow rate of secondary flow is independent from condensing pressure. Only the increase of evaporating pressure can raise the secondary flow rate. That is why there is a horizontal part at left side of the line. When condensing pressure is higher than critical pressure, the mixed flow is no longer choked and the secondary mass flow varies with condensing pressure. The higher the condensing pressure is, the more resistance there will be at the outlet of ejector. The pressure difference between ejector inlet and outlet that generates motive force is reduced. So the entrainment ratio decreases sharply as a result. Moreover, continually increasing condensing pressure will cause reverse flow circumstance in ejector which should be highly prohibited. Also from Fig.6, it can be found that when evaporating pressure increases, both entrainment ratio and critical pressure value increase. Since the increment of evaporator pressure leads to the increase of pressure difference between secondary inlet and vacuum region, more secondary flow will be sucked into ejector due to this larger pressure difference. Thus the entrainment ratio increases with increase of evaporator pressure. Besides, the evaporator pressure augment results in larger momentum that is capable of dealing with higher condensing pressure. Hence, when evaporator pressure increases, the critical pressure value will increase that offers a wider and safer operation range for condenser. So the increases of evaporating pressure will result in a better performance of ejector with sacrifice of evaporator operation range.

The variation of entrainment ratio with the condensing pressure under constant evaporating pressure is illustrated in Fig. 7. It is observed that 1) under constant evaporating pressure, increasing generating pressure causes entrainment ratio to decrease and 2) critical pressure value will increase with increment of generating pressure. The reason for this phenomenon is obvious that when generating pressure increases, the primary mass flow rate will increase. Since the diameter of mixing chamber is fixed and the mixed flow is choked within mixing chamber when condensing pressure lower than critical value, an increment of primary flow rate will cause secondary flow rate to decrease which leads to a reduction of entrainment ratio. The numerator which represents secondary flow rate decreases and the denominator which represents primary flow increases, together the entrainment ratio decreases. As secondary flow goes through evaporator and related to cooling capacity, this also leads to a decrease of cooling capacity and COP. However, a higher generating pressure will causes the momentum of the mixed flow to increase. Thus, the critical condenser pressure is increased. Higher generating pressure requires more power from liquid pump or higher temperature produced by generator heater. In terms of system efficiency, it is beneficial to have the system operated under lower generating pressure.

Both Fig.6 and Fig.7 indicate that the entrainment ratio of ejector A is higher than that of ejector B under same operating conditions. The reason for this performance is that the mixing chamber diameter of ejector B is 6mm which is 76.4% larger than 3.4mm of ejector A while the nozzle throat diameter of ejector B is 3mm which is 87.5% bigger than 1.6mm of ejector A. So under the same operating conditions, the ejector B ought to be able to entrain more secondary flow due to larger nozzle throat, however, since the mixing chamber diameter of ejector B is only 76.4% increase from A, this will limit the mass flow rate of secondary flow. As a result, both primary flow and secondary flow will increase when applying ejector B, the increment amount of primary flow is higher than that of secondary flow which leads to decrease of entrainment ratio.

For better performance, the ejector with higher entrainment ratio is desired. Thus, ejector A is chosen to conduct the following experiments.

#### 348 *B. Effect of primary and secondary pressure on entrainment ratio*

349 The evaporating pressure on system performance is tested for both entrainment ratio and COP. Fig.8 depicts how the  
350 entrainment ratio varies with evaporating pressure.

351 From the figure, it can be concluded that for the constant condensing and generating pressures, the entrainment ratio increases  
352 along with the evaporating pressure. With the increase of evaporating pressure, the pressure difference between ejector secondary  
353 inlet and vacuum region increases, thus a small amount of primary motive flow is sufficient to generate enough suction force which  
354 entrains the secondary flow into ejector. Therefore, at higher evaporating pressure value, the entrainment ratio is larger. On the  
355 other hand, an increase of generating pressure will cause the entrainment ratio to decrease. Similar trend can be observed from  
356 variation of COP with evaporating pressure which will be shown later.

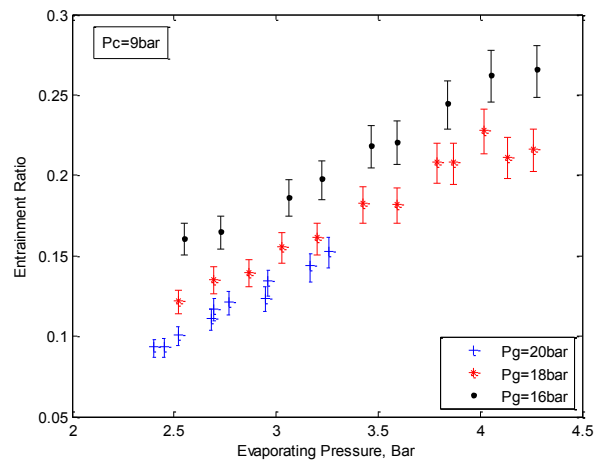


Fig. 8. Variation of entrainment ratio with evaporating pressure under constant condensing pressure

In order to investigate the relationship between system performance and generating pressure, the experiment is conducted under following conditions: the  $P_c$  is constant at 9 bar, the  $P_e$  is constant at 3 and 4 bar while the  $P_g$  is varied from 10–23 bar and the system is operating under hybrid mode.

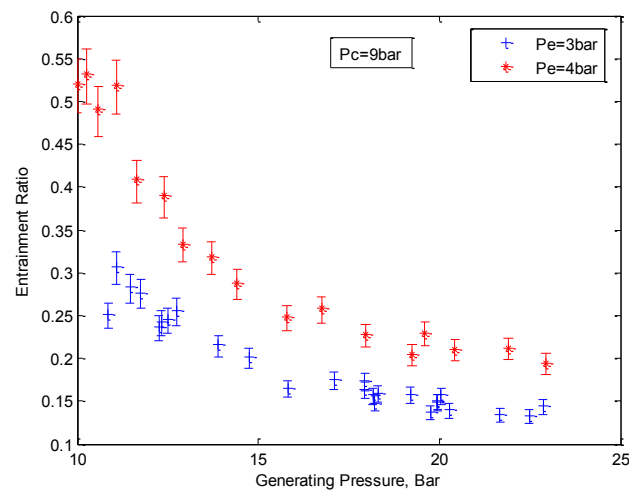


Fig. 9. Variation of entrainment ratio with generating pressure under constant condensing pressure

The variation of entrainment ratio with generating pressure under constant condensing pressure is illustrated in Fig. 9. It can be seen that the entrainment ratio under hybrid mode is decreasing along with the increasing of generating pressure. Since under hybrid mode, compressor helps compensate suction effect even when generating pressure is not high enough. Although the entrainment ratio seems to be quite satisfying, it is due to the small primary mass flow rate, the actual cooling capacity is not at its optimum. As generating pressure keeps increasing, both the primary mass flow rate and the suction effect generated by ejector are increasing proportionally; this will help mitigate the compressor loads which in turn reduce the power consumption of compressor.

### C. Effect of different pressure on COP

Since COP is an important parameter to evaluate the system performance and also in order to improve the efficiency of the system, the influence of evaporating and generating pressure on COP is studied. The condensing pressure is not studied because its adjustment is not practical as previous two pressures in real application.

From the experiment data, it can be seen that COP increases with the increment of evaporating pressure under all three generating pressures. From previous results, it is known that increase of evaporator pressure leads to increase of entrainment ratio and finally results in cooling capacity augment. Also, under constant generating and condensing pressure, a higher evaporating pressure is able to be entrained by a lower generating pressure which means higher evaporating pressure requires lesser power consumption of liquid pump or generator heater. This will together help improve the COP of the system. In order to achieve higher COP value, the system should be run at higher evaporating pressure condition. However, in real application, a lower evaporating temperature, which also means lower evaporating pressure, is desired. So it has to be a balance between achieving higher COP and desired evaporating temperature.

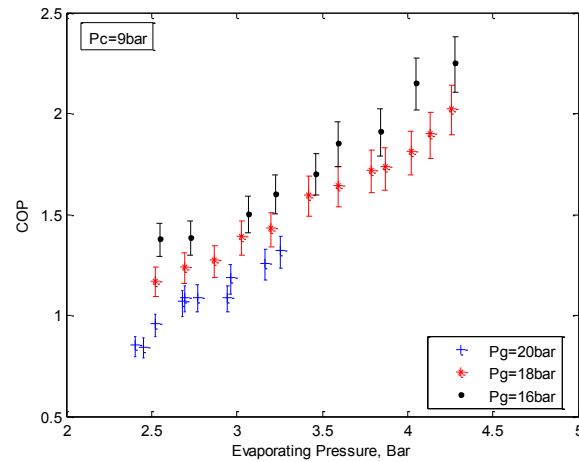


Fig. 10. Variation of COP with evaporating pressure under constant condensing pressure

Additionally, the variation of COP with generating pressure is investigated. Under hybrid mode, for given evaporating and condensing pressure, COP is increasing with the increment of generating pressure. Although the entrainment ratio is decreasing with the increment of generating pressure, it does not mean that COP will follow the same pattern. At higher generating pressure, the mass flow rate of primary flow is higher; the suction force generated by primary flow is large enough to achieve sufficient entrainment effect under relative lower secondary pressure condition. Thus the compression ratio decreases which leads to a reduction in compressor power consumption. If more exhaust heat is collected and recovered, the generating pressure is higher which results in a higher COP.

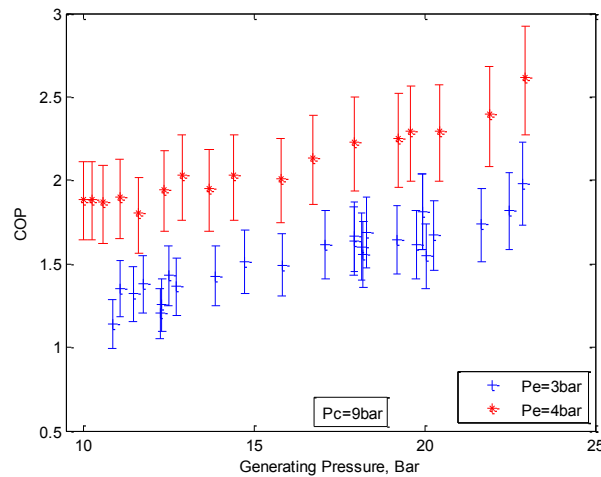
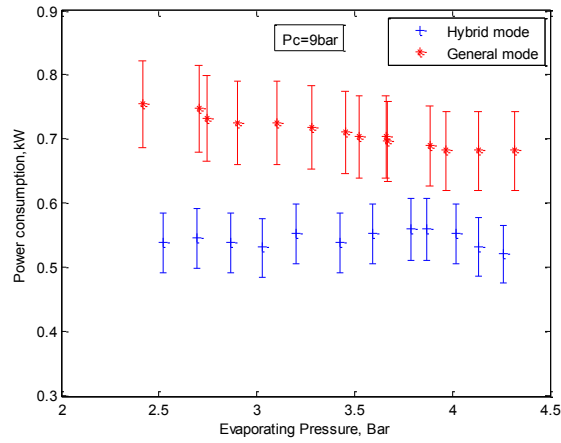


Fig. 11. Variation of COP with generating pressure under constant condensing pressure

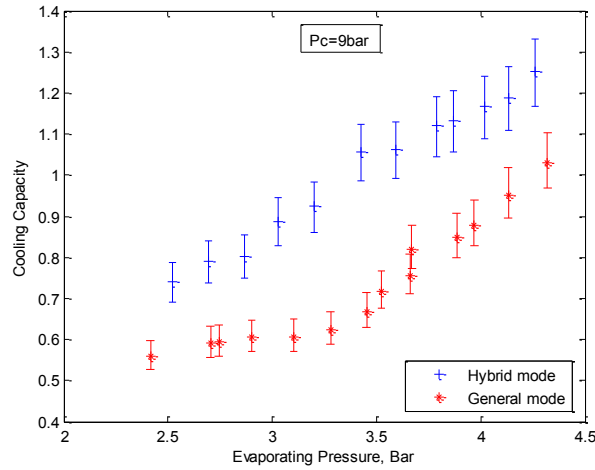
#### D. Performance comparison between two modes

The comparison of cooling capacity, power consumption and COP between general mode and hybrid mode are illustrated in Fig. 12, 13, 14, respectively. From the three figures, it can be seen that the application of ejector in hybrid refrigeration cycle (hybrid mode) can indeed improve the system performance over conventional vapor compression cycle (general mode). From equation (16) and (17), it can be observed that there are two more power consumed components (liquid pump and generator heater) within hybrid mode. However, the power consumption of hybrid mode is lower than that of general mode. The reason is that the employment of passive device like ejector which utilizes the waste heat energy to generator suction force shares part of the responsibility of the compressor, particularly, the operation principle of mixing chamber in some extent are similar to a compressor which reduces the energy consumption of mechanical compressor in return. This reduced amount of energy is larger than the power consumption which liquid pump and heater bring along. Thus, the total power consumption of hybrid mode is lower than that of general mode. Additionally, the use of ejector enhances the entrainment effect of secondary flow that related to cooling capacity. Therefore, the cooling capacity of hybrid mode is higher than that of general mode. All these factors together contribute to the COP improvement of hybrid refrigeration system. Given a scrutiny towards the result, it can be found that the cooling capacity is averagely 27.3% higher under hybrid mode than that of general mode; the power consumption is averagely 20.3% lesser under hybrid mode. As a consequence, the COP improvement of hybrid mode is about 34% which meets the rough estimation; however, there still remains a distance from setting goal. Since ejector is capable of utilizing waste source energy and this kind of energy is

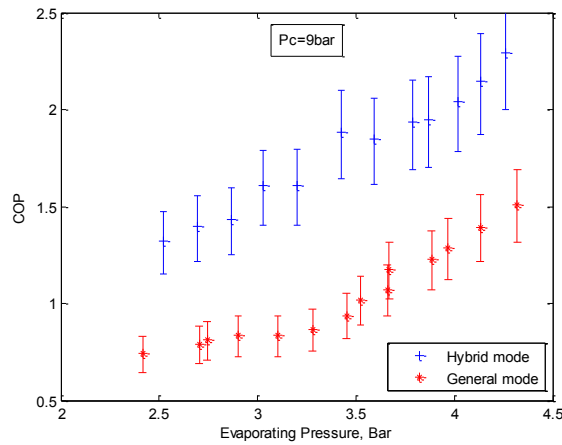
409 free in a sense. If the generator heater of proposed system is powered by low grade heat energy, such as automobile exhaust,  
410 geothermal or solar energy, the power consumption of system will be further reduced. Thus 34% improvement is not the ultimate  
411 goal. The improvement can also be realized from an appropriate control strategy and optimization algorithm which will be studied  
412 in the future.



413  
414 Fig. 12. Power consumption between hybrid mode and general mode



415  
416 Fig. 13. Cooling capacity between hybrid mode and general mode



417  
418 Fig. 14. COP between hybrid mode and general mode

419 V. CONCLUSIONS

420 In this work, the effect of geometrical parameter on ejector performance and the effect of condenser, evaporator and generator  
421 pressure on the hybrid system performance was investigated experimentally. The performance comparison between general mode

and hybrid mode was presented. Two performance indexes namely COP and entrainment ratio, were introduced to evaluate the performance improvement of the hybrid ejector-based air conditioning system. The primary findings are as follows:

- 1) The performance of ejector is sensitive to its area ratio and an ejector with area ratio of 4.51 gives better performance than the one of 4 in terms of critical pressure and entrainment ratio.
- 2) The performance of hybrid system is sensitive to evaporating and generating pressure. A higher evaporating pressure leads to larger entrainment ratio and COP while a higher generating pressure only results in higher COP.
- 3) The compressor applied which enlarge the pressure difference between ejector secondary inlet and evaporator outlet indeed improve the overall performance and the COP improvement can reach up to 34% which indicated the potential of energy saving in hybrid ejector refrigeration system.

#### ACKNOWLEDGMENT

This work was supported by National Research Foundation of Singapore under the grant NRF2011 NRF-CRP001-090.

#### REFERENCES

- [1] Liao Yuhang. Performance analysis on a solar-driven air-cooled ejector refrigeration system for air-conditioning using ammonia as refrigerant. *Applied Mechanics and Materials* 2014;501-504:2282-2287.
- [2] R'mierciew, K. Experimental investigations of solar driven ejector air-conditioning system. *Energy and Buildings* 2014;80:260-267.
- [3] Bin-Juine Huang. Performance test of solar-assisted ejector cooling system. *International Journal of Refrigeration* 2014;39:172-185.
- [4] Sumeru, Martin, L. Energy savings in air conditioning system using ejector: an overview. *Applied Mechanics and Materials* 2014;493:93-98.
- [5] Tirmizi, S.A. Performance analysis of an ejector cooling system with a conventional chilled water system. *Applied Thermal Engineering* 2014;66:113-121.
- [6] Jiautheen, P.B. Annamalai, M. Review on ejector of vapor jet refrigeration system. *International Journal of Air-conditioning and Refrigeration* 2014;22:143-173.
- [7] Fang Liu; Groll, E.A. Study of ejector efficiencies in refrigeration cycles. *Applied Thermal Engineering* 2013;52:360-370.
- [8] Al-Alili, A; Yunho Hwang. Review of solar thermal air conditioning technologies. *International Journal of Refrigeration* 2014;39:4-22.
- [9] Khaliq, A. Performance analysis of a waste-heat-powered thermodynamic cycle for multi-effect refrigeration. *International Journal of Energy Research* 2015;39:529-542.
- [10] Pounds D.A, Dong J.M, Cheng P, Ma H B. Experimental investigation and theoretical analysis of an ejector refrigeration system. *International Journal of Thermal Sciences* 2013;67:200-209.
- [11] Yin Hai Zhu, Peixue Jiang. Hybrid vapor compression refrigeration system with an integrated ejector cooling cycle. *International Journal of Refrigeration* 2012;35:68-78.
- [12] Yan Jia, Wenjian Cai, Yanzhong Li. Geometry parameters effect for air-cooled ejector cooling system with R134a refrigerant. *Renewable energy* 2012;46:155-163.
- [13] Yan Jia, Wenjian Cai. Area ratio effects to the performance of air-cooled ejector refrigeration cycle with R134a refrigerant. *Energy Conversion and Management* 2012;53:240-246.
- [14] Chen Jianyong, Havtun Hans and Palm Bjorn. Investigation of ejectors in refrigeration system: Optimum performance evaluation and ejector area ratios perspectives. *Applied Thermal Engineering* 2014;64:182-191.
- [15] Wang F, Shen S Q, Li D Y. Evaluation on environment-friendly refrigerants with similar normal boiling points in ejector refrigeration system. *Heat and mass transfer* 2014;51:965-972.
- [16] Besagni Giorgio, Mereu Riccardo, Di Leo, Giuseppe, Inzoli Fabio. A study of working fluids for heat driven ejector refrigeration using lumped parameter models. *International Journal of Refrigeration* 2015;58:154-171.
- [17] Boumaraf Latra, Haberschill Philippe. Investigation of a novel ejector expansion refrigeration system using the working fluid R134a and its potential substitute R1234yf. *Energy economics* 2014; 45:148-159.
- [18] Chen Lin, Yanzhong Li, Wenjian Cai, Jia Yan, Yu Hu. Experimental investigation of the adjustable ejector in a multi-evaporator refrigeration system. *Appl Therm Eng* 2013;61:2-10.
- [19] Meibo Xing, Gang Yan, Jianlin Yu. Performance evaluation of an ejector subcooled vapor-compression refrigeration cycle. *Energy Conversion and Management* 2015;92:431-436.
- [20] Huang BJ, Wu JH, Hsu HY, Wang JH. Development of hybrid solar-assisted cooling/heating system. *Energy Conversion and Management* 2010;51:1643-50.
- [21] Huang BJ, Petrenko VA, Chang JM, Lin CP and Hu SS. A combined-cycle refrigeration system using ejector cooling cycle as the bottom cycle. *International Journal of Refrigeration* 2001;24:391-9.
- [22] Ersoy H.K, Billir Sag N. Preliminary experimental results on the R134a refrigeration system using a two-phase ejector as an expander. *International Journal of Refrigeration*, 2014; 43: 97-110.
- [23] Korn. *Mathematical handbook for scientists and engineers*. Dover 2000: 134.
- [24] Kanjanapon Chunnanond, Satha Aphomratana. Ejector: application in refrigeration technology. *Renewable and sustainable energy reviews* 2004;8:129-155.
- [25] Xudong D, Wenjian Cai and Jia L. A hybrid modeling for the real-time control and optimization of compressors. In: 2009 4<sup>th</sup> IEEE Conference on Industrial Electronics and Application, ICIEA 2009, May 25-27, Xi'an, China, pp.3256-3261.
- [26] Xudong D, Wenjian Cai and Lei Zhao. Evaporator modeling—a hybrid approach. *Appl Therm Eng* 2009;86:81-8.
- [27] Huang BJ, Chang JM, Wang CP, Petrenko VA. A 1-D analysis of ejector performance. *Int J Refrigeration* 1999;22:354-364.
- [28] Yin Hai Zhu, Wenjian Cai. Shock circle model for ejector performance evaluation. *Energy Conversion and Management* 2007;48:2533-2541.